The FASEB Journal

Purification of mitochondria from skeletal muscle tissue for transcriptomic analyses reveals localization of nuclear-encoded noncoding RNAs

Jessica Silver[1] | Adam J. Trewin[1,2] | Stella Loke[3] | Larry Croft[3] | Mark Ziemann[4,5] | Megan Soria[4] | Hayley Dillon[1,6] | Søren Nielsen[7] | Séverine Lamon[1] | Glenn D. Wadley[1]

[1]Institute for Physical Activity and Nutrition, School of Exercise and Nutrition Sciences, Deakin University, Geelong, Victoria, Australia

[2]Department of Anatomy and Physiology, University of Melbourne, Melbourne, Victoria, Australia

[3]Genomics Centre, School of Life and Environmental Sciences, Deakin University, Geelong, Victoria, Australia

[4]School of Life and Environmental Sciences, Deakin University, Geelong, Victoria, Australia

[5]Burnet Institute, Melbourne, Victoria, Australia

[6]Human Integrated Physiology and Sports Cardiology Laboratory, Baker Heart and Diabetes Institute, Melbourne, Victoria, Australia

[7]The Centre of Inflammation and Metabolism and the Centre for Physical Activity Research, Rigshospitalet, University of Copenhagen, Copenhagen, Denmark

Correspondence
Glenn D. Wadley, Institute for Physical Activity and Nutrition, School of Exercise and Nutrition Sciences, Deakin University, Geelong, VIC 3125, Australia.
Email: glenn.wadley@deakin.edu.au

Abstract

Mitochondria are central to cellular function, particularly in metabolically active tissues such as skeletal muscle. Nuclear-encoded RNAs typically localize within the nucleus and cytosol but a small population may also translocate to subcellular compartments such as mitochondria. We aimed to investigate the nuclear-encoded RNAs that localize within the mitochondria of skeletal muscle cells and tissue. Intact mitochondria were isolated via immunoprecipitation (IP) followed by enzymatic treatments (RNase-A and proteinase-K) optimized to remove transcripts located exterior to mitochondria, making it amenable for high-throughput transcriptomic sequencing. Small RNA sequencing libraries were successfully constructed from as little as 1.8 ng mitochondrial RNA input. Small RNA sequencing of mitochondria from rat myoblasts revealed the enrichment of over 200 miRNAs. Whole-transcriptome RNA sequencing of enzymatically purified mitochondria isolated by IP from skeletal muscle tissue showed a striking similarity in the degree of purity compared to mitoplast preparations which lack an outer mitochondrial

Abbreviations: Cq, Quantitative cycle; DE, differentially expressed; ER, endoplasmic reticulum; FDR, false discovery rate; IP, Immunoprecipitation; IMS, mitochondrial intermembrane space; IMM, inner mitochondrial membrane; lncRNA, long non-coding RNA; miRNA, microRNA; mtDNA, mitochondrial DNA; ncRNA, non-coding RNA; nDNA, nuclear DNA; OMM, outer mitochondrial membrane; OXPHOS, oxidative phosphorylation; qPCR, quantitative PCR; RIN, RNA integrity number; RNA-seq, NA sequencing; RNase, ribonuclease; sRNA, small RNA.

Jessica Silver and Adam J. Trewin co-first authors.

membrane. In summary, we describe a novel, powerful sequencing approach applicable to animal and human tissues and cells that can facilitate the discovery of nuclear-encoded RNA transcripts localized within skeletal muscle mitochondria.

1 | INTRODUCTION

Mitochondria are subcellular organelles essential for numerous cellular processes including energy metabolism, signaling, ion and redox homeostasis, and regulation of apoptosis.[1] Mitochondria are comprised of proteins encoded by both the nuclear and mitochondrial genomes, but nuclear-encoded RNAs are not usually localized within mitochondria. A small number of specific nuclear-encoded noncoding RNAs (ncRNAs), such as microRNAs (miRNAs)[2–4] and possibly long noncoding RNAs (lncRNAs),[5] can however be imported into mitochondria.[6] This may occur via the polynucleotide phosphorylase[7] and other putative transport mechanisms (reviewed in Silver et al.).[6] Because ncRNAs have the ability to regulate various transcriptional and translational processes relating to mitochondrial function, it is of interest to determine which of these may localize within mitochondria in order to understand the nature of their potential regulatory actions.

Investigations into mitochondria-localized nuclear-encoded RNAs have been constrained, first, by the technical challenges of obtaining pure mitochondrial preparations free of confounding RNAs peripheral to isolated mitochondria and, second, by the significantly lower RNA yields from subcellular fractions when compared to whole tissue homogenates. Early studies providing evidence for the localization of ncRNAs within mitochondria stem from micro-array analysis and were routinely validated by single qPCR assays or in situ hybridization.[2–4] However, the overall population of ncRNAs that localize within mitochondria and their regulatory actions, particularly within metabolically active tissues, remains largely unknown.

Skeletal muscle constitutes ~40% of human body mass and plays a central role in whole body metabolism.[8] To meet these dynamic bioenergetic demands, skeletal muscle is densely populated with mitochondria.[9] Thus, gaining a greater understanding of the RNA profile within muscle mitochondria may yield important insights into the cellular biology and etiology of diverse metabolic diseases characterized by mitochondrial dysfunction, such as diabetes mellitus and chronic myopathies.[6] Here, we report a method for isolating and optimizing the enzymatic purification of mitochondria from rodent muscle cells or tissues. We provide direct evidence for the purity of this mitochondrial fraction, making it amenable for downstream high-throughput analyses. We also describe methods for small RNA and whole-transcriptome sequencing of mitochondria isolated from cultured myoblasts as well as skeletal muscle tissue samples from animals and humans.

2 | MATERIALS AND METHODS

2.1 | Cell culture

L6 rat myoblast cells were obtained from a commercial vendor (ATCC Cat# CRL-1458, RRID: CVCL_0385). Cells were cultured at 37°C with 5% CO_2 in a humidified incubator in media consisting of Dulbecco's Modified Eagle Medium (DMEM; Gibco #11995-065) supplemented with 10% v/v FBS (Gibco #A3161001), 100 U/mL penicillin, and 100 μg/mL streptomycin (Gibco #15140-122). Cells were grown in 150 mm dishes to ~90% confluence and then washed with sterile PBS and detached (Gibco TrypLE Express #LTS12604021). Cells used for all experiments were ≤9 passages from stock and tested negative for mycoplasma contamination (Agilent MycoSensor QPCR Assay Kit, 302107).

2.2 | Myoblast mitochondrial isolation

Mitochondria were isolated from L6 myoblasts via immunoprecipitation (Miltenyi Biotec #130-096-946). Briefly, ~5×10^6 cells (suspended in a small volume of PBS after detachment) were transferred to 1 mL ice-cold lysis buffer on ice and then mechanically homogenized with 20 passes in a 7-mL glass dounce homogenizer (#357542, Wheaton, NJ). Wash buffer (9 mL) was added to the lysate and transferred to a falcon tube. Anti-TOMM22 antibody-conjugated magnetic beads (50 μL) were added to the 10 mL lysate and incubated with gentle inversion for 1 h at 4°C. Lysate was passed through a pre-separation filter and then flowed through a column mounted on a magnetic rack. Mitochondria were washed 3 times prior to elution. Mitochondria were pelleted via centrifugation at 13 000 g for 2 min at 4°C. Supernatant was then removed and the mitochondrial pellet resuspended in storage buffer to be used for subsequent enzymatic purification steps described below.

2.3 | Enzymatic purification of myoblast mitochondria

Protease treatment: To remove proteins not localized within intact mitochondria, aliquots of isolated

mitochondria (1 μg total protein each) were incubated in a 50 μL reaction with or without Triton X-100 (1% v/v) and with or without proteinase-K (Qiagen #19131, final concentration 20 μg/mL) for 15 min at room temperature. Phenylmethylsulfonyl fluoride (20 mM) was added to inhibit proteinase-K. Samples were then stored at −20°C until immunoblot analysis.

RNase treatment: To remove RNA not localized within intact mitochondria, in a 50 μL reaction, aliquots of isolated mitochondria (1 μg total protein each) first had 100 ng mRNA spike-in control added (StemMACS eGFP mRNA #130-101-114, Miltenyi Biotec) and were then incubated with or without Triton X-100 (1% v/v) and with or without RNase-A (Qiagen #19101, final concentration range 1–1000 μg/mL) and incubated on ice for 30 min. TRIzol reagent was then added to simultaneously inactivate RNase activity, lyse mitochondria, and preserve RNA. Samples were then stored in TRIzol at −20°C until RNA isolation.

2.4 | Immunoblot analysis

Mitochondrial samples were resuspended in RIPA buffer (Millipore #20-188) containing protease inhibitors (Sigma #P8340). Protein concentration was determined by BCA assay (Pierce #23225). Samples were mixed with reducing loading buffer (4× Laemmli sample buffer with 10% 2-mercaptoethanol). Samples were loaded into a 4%–15% gel (Bio-Rad #5678085) in addition to molecular weight marker (Bio-Rad #161-0373), which were then separated by electrophoresis. The stain-free gel was UV-activated for 1 min and imaged for total protein (Bio-Rad Chemi Doc XR+, Hercules, CA, USA) with Image Lab software (Bio-Rad Image Lab v6). Protein was then transferred to a methanol-soaked polyvinylidene difluoride (PVDF) membrane (Millipore Immobilon FL 0.45 μm #IPFL00010). The membrane was then PBS-washed and then blocked for 1 h (Li-Cor Intercept PBS blocking buffer). The membrane was then incubated with primary antibody in blocking buffer +0.2% v/v Tween-20 overnight at 4°C. Primary antibodies used were as follows: anti-TOMM20 (Abcam #ab186735; 1:1000), anti-Cytochrome-c (Abcam #ab133504; 1:1000), anti-Citrate Synthase (Cell Signaling Technology #14309; 1:1000), anti-α-Tubulin (Cell Signaling Technology #3873; 1:1000), anti-mitofilin (Abcam #ab110329; 1:1000), anti-AIF (Cell Signaling Technology #4642, 1:500), anti-catalase (Abcam #ab1877, 1:500), anti-S6 RPL (Cell Signaling Technology #2217, 1:1000), anti-GM130 (BD Transduction Laboratories #610822, 1:1000), anti-SERCA1 (Cell Signaling Technology #4219, 1:1000), and anti-Lamin B1 (Cell Signaling Technology #12586;

1:1000). Membranes were then washed with PBST and incubated with secondary antibodies (Cell Signaling Technology) anti-rabbit or anti-mouse IgG Dylight® 680 nm (Cell Signaling Technology #5366S, #5470S) or 800 nm (Cell Signaling Technology #5151S or #5257S) at 1:10 000 in blocking buffer containing 0.2% Tween-20 and 0.01% SDS for 1 h at room temperature. Fluorescent signal was then digitally acquired (Licor Odyssey® Infrared Imaging System, Lincoln, NE, USA).

2.5 | RNA isolation and quality control

Myoblast mitochondria samples stored in TRIzol were thawed on ice and centrifuged at 10 000 g for 10 min at 4°C. An aliquot of the supernatant was then used for RNA purification with on-column DNase-I treatment (Direct-zol RNA MicroPrep R2060, Zymo Research). RNA concentration and purity were determined by spectrophotometry (NanoDrop 1000, Thermo Fisher Scientific), while RNA fragment size distribution was assessed by gel electrophoresis (TapeStation HS-RNA, Agilent Technologies).

2.6 | Reverse transcription and quantitative PCR (RT-qPCR)

Equal volumes of isolated RNA from the RNase-treated mitochondria samples (to account for differences in total RNA yield between samples due to RNase treatment) were reverse-transcribed to first-strand cDNA in a 20 μL reaction along with no-template and no-RTase controls (Applied Biosystems High Capacity RT kit #4368814). Quantitative PCR was performed in triplicate (Agilent AriaMX G8830A) on 4 ng of cDNA in a 10 μL reaction consisting of SYBR green master mix (Applied Biosystems #4367659) with 0.3 μM forward and reverse primers (Table 1).

Thermal conditions used for qPCR were 10 min at 95°C (activation) and then 40 cycles of 15 s at 95°C (denature) and 60 s at 55–60°C (anneal/extend). A dissociation curve was performed to confirm the amplification of a single product. Quantification cycle (C_q) thresholds were calculated using software (Agilent Aria v1.5).

2.7 | Myoblast small RNA sequencing and bioinformatics

Total RNA isolated from individual ($n = 7$) L6 mitochondria samples was pooled into a single tube, from which serial dilutions ranging from 0.3 to 20 ng/μL were

TABLE 1 List of RT qPCR primers.

Target	Forward (5′-3′)	Reverse (5′-3′)	Accession ID
Mt-co3	GACGGAATTTACGGCTCAACAT	AATTAGGAAAGTTGAGCCAATAATTACG	>NC_001665.2 Rattus norvegicus strain BN/SsNHsdMCW mitochondrion, complete genome
Cox4i1	GTGCTGATCTGGGAGAAGAGCTA	GGTTGACCTTCATGTCCAGCAT	>NM_017202.1 Rattus norvegicus cytochrome c oxidase subunit 4i1 (*Cox4i1*), mRNA; nuclear gene for mitochondrial product
eGFP	ACTTCTTCAAGTCCGCCATG	AGCTCGATGCGGTTCACCAG	>XM_013480425.1 Eimeria maxima Green fluorescent protein, related partial mRNA

prepared. cDNA libraries were then prepared using a range of mitochondrial RNA inputs (final input range 1.8–120 ng) using the NEBNext Multiplex Small RNA Library Prep Set (New England Biolabs). To investigate the efficiency of small RNA library preparation across a range of mitochondrial RNA inputs, libraries were prepared either according to the manufacturer's recommendations for low RNA inputs (NEBNext 3′ and 5′ SR Adaptors, and RT primer for Illumina diluted 0.5X, 15 PCR cycles) or with modifications (NEBNext 3′ and 5′ SR Adaptors, and RT primer for Illumina diluted 0.3× or 0.1×, 20 PCR cycles). cDNA concentration was determined by fluorometric quantitation (Qubit 1xds-DNA, Thermo Fisher Scientific), while cDNA fragment size distribution was assessed by gel electrophoresis (TapeStation HS-D1000, Agilent Technologies).

An equimolar pool of all uniquely indexed small RNA libraries was prepared. Twenty-five μL of the equimolar pool was loaded across two lanes on a 6% Novex TBE polyacrylamide gel (Thermo Fisher Scientific), with 5 μL Quick-Load pBR322 DNA-MspI Molecular Marker (New England Biolabs Inc.) in a separate lane. The buffer dam was filled with 600 mL 1X TBE running buffer and the gel run at 120 V for 1 h. The gel was then incubated with 50 mL 1X TBE spiked with 1X SYBR Gold Nucleic Acid Gel Stain (Thermo Fisher Scientific), before being visualized on a Safe Imager 2.0 Blue-Light Transilluminator (Invitrogen) following exposure to UV-Blue (470 nm) light. Fragments corresponding to the 130–160 bp region were manually excised, before suspended and then crushed in 250 μL gel elution buffer (New England Biolabs Inc.). To increase the recovery of low concentrations of small nucleic acids, cDNA was precipitated overnight at −20°C with 0.3 M sodium acetate (pH 5.5), 4× volumes of 100% ethanol, and 1 μL linear acrylamide carrier. Following overnight precipitation, the solution was centrifuged at 16 000 g for 60 min to pellet the cDNA fragment. The cDNA pellet was washed twice with 80% ethanol and resuspend in 12 μL TE buffer. Fragment size

distribution of the gel-extracted cDNA pool was assessed by gel electrophoresis (TapeStation HS-D1000, Agilent Technologies).

RNA sequencing was performed by the Deakin University Genomics Core on the Illumina MiniSeq platform. A 1.3 pM loading pool was prepared with 20% Phi-X spike-in and was sequenced on a single-end 75 bp run. Sequenced reads underwent quality checks with FastQC before the adapter and reads <20 nt were trimmed. Small RNAs, including miRNAs, are not well sequenced in the rat genome but are conserved between rat and mouse species. Reads were mapped to known mature mouse miRNAs accessible from miRbase v22.0. Raw read counts were normalized by the size of each individual library. Counts were visualized using GraphPad Prism (v7).

2.8 | Rodent study ethical approval and procedures

All experimental procedures were approved by the Deakin University Animal Ethics Committee (G02-2019). All animals were housed and treated in accordance with standards set by Deakin University's Animal Welfare Committee, which complies with the ethical and governing principles outlined in the Australian code for the care and use of animals for scientific purposes. Wistar Kyoto male rats were obtained from the Animal Resource Centre, Perth, Western Australia. Rats were housed in pairs and maintained with a 12-h light/dark cycle, constant temperature of $21 \pm 2°C$, and humidity levels between 40% and 70%. Rats had ad libitum access to standard chow diet and tap water. At 9 weeks of age, animals were humanely killed following dissection of the heart under heavy anesthesia using 5% isoflurane gas. The gastrocnemius muscle was rapidly excised, and then, the inner red portion was dissected. A portion of this was snap-frozen in liquid nitrogen for subsequent whole muscle RNA analyses, and a separate ~100 mg piece was taken for mitochondrial isolation.

2.9 | Rat muscle tissue mitochondrial isolation

Tissue was immediately placed in 1 mL ice-cold lysis buffer containing 5 μL/mL protease inhibitors (Sigma #P8340) and minced using fine scissors before mechanical homogenization with an ice-cold Teflon-tipped glass dounce homogenizer (10 passes with rotation at 350 rpm). Intact mitochondria were then isolated using the magnetic-bead immunoprecipitation method as described above for L6 myoblasts except with the following RNase treatment conditions: RNase-A 340 μg/mL in a reaction with ~20 μg total mitochondrial protein performed for 1 h at 37°C, after which 5 μL proteinase-K (stock concentration 600 mAU/mL) was then added to inactivate RNase activity.[2] Each tube was briefly inverted before the mitochondria solutions were then centrifuged at 8000 g for 10 min at 4°C. The supernatant was aspirated, and the pellet was washed twice with 100 μL ice-cold storage buffer. The RNase-treated mitochondrial pellet was resuspended in 100 μL storage buffer and then frozen at −80°C until RNA extraction.

2.10 | Rat muscle tissue and isolated mitochondria RNA extraction

For RNA extraction from gastrocnemius whole muscle tissue, ~15 mg frozen tissue was placed in a liquid nitrogen prechilled cryotube with a 5-mm stainless steel bead. The tissue was then mechanically disrupted (2 cycles at 4 m/s for 10 s, MP Biomedical FastPrep). Tri-reagent (600 μL) was added and then RNA extracted (Zymo Directzol RNA Miniprep #R2050). For RNA extraction from isolated mitochondria from the respective red portion of gastrocnemius muscle, frozen samples were thawed in the presence of 5 volumes of TRI-reagent (Qiagen), pipette mixed thoroughly, and then centrifuged at 16 000 g for 1 min. RNA extraction was then performed with on-column DNase I treatment (Zymo Research Direct-zol RNA MicroPrep #2060). Extracted RNA was tested for purity on NanoDrop, and concentration with Qubit HS RNA assay (Thermo Fisher) and then RNA integrity number (RIN) were determined using a TapeStation (Agilent) with High Sensitivity RNA reagents. All RINs from whole tissue RNA were ≥7.0.

2.11 | Rat muscle tissue and isolated mitochondria total RNA sequencing

Total RNA from whole tissue (50 ng) and isolated mitochondria (10 ng) was converted to cDNA libraries (Zymo-Seq RiboFree Total RNA #R300, Zymo Research). Briefly, ribosomal RNA was depleted and then remaining transcripts were fragmented and converted to cDNA using random priming. After second-strand synthesis, the ends of the cDNA were enzymatically repaired and Illumina-compatible sequencing adaptors were ligated. Library size (TapeStation, Agilent) and concentration (Qubit) were assessed prior to sequencing. RNA sequencing was performed by the Deakin University Genomics Core on the Illumina NovaSeq 6000 platform. Reads underwent adapter trimming and quality check with Skewer then mapped to the rat genome (Ensembl version 99) with STAR aligner v2.7.2a. STAR-generated read counts were collated in R version 4.0.3 (R Development Core Team, 2010). Normalized counts were visualized using GraphPad Prism (v7). Analysis of differential expression was performed using Voom/Limma in Degust v 4.1.5.[10] Transcripts with a false discovery rate (FDR) <0.05 were considered differentially expressed.

2.12 | Rat muscle tissue mitoplast preparation and RNA sequencing

All experimental procedures were approved by the Deakin University Animal Ethics Committee (G01-2023) and housed and treated in accordance with standards set by Deakin University's Animal Welfare Committee, which complies with the ethical and governing principles outlined in the Australian code for the care and use of animals for scientific purposes. A 14-week-old male Wistar Kyoto rat was obtained from the Animal Resource Centre, Perth, Western Australia, and humanely killed following dissection of the heart under heavy anesthesia using 5% isoflurane gas. The hindlimb muscles were rapidly excised and cut into 200 mg pieces. Each piece was immediately placed in 1 mL ice-cold lysis buffer containing 5 μL/mL protease inhibitors (Sigma #P8340), minced using fine scissors, and incubated on ice for 30 min. Samples were then mechanically homogenized with an ice-cold Teflon-tipped glass dounce homogenizer (10 passes with rotation at 350 rpm), and the homogenate was pooled. To compare different isolation methods, intact mitochondria were then isolated from separate aliquots of the same homogenate using either the magnetic-bead immunoprecipitation method described above or a differential centrifugation method.

To obtain mitochondria by differential centrifugation, tissue homogenate was spun at 800 g for 10 min at 4°C and the pellet was discarded. The supernatant was then spun at 16 000 g for 30 min at 4°C and the pellet resuspended in 1 mL of isolation buffer containing 1 mM PMSF and then

spun at 10 000 g for 10 mins at 4°C. The mitochondrial pellets were washed twice in 1 mL ice-cold storage buffer. The mitochondrial pellets were then pooled and resuspended a small volume of storage buffer.

To generate mitoplasts, intact mitochondria (40 μg) obtained from the magnetic-bead immunoprecipitation method were incubated in 0.06% digitonin on ice for 30 min, followed by 30-min incubation on ice with proteinase-K (final concentration 20 μg/mL). The samples were then incubated on ice for 10 min in PMSF (final concentration 10 mM) to inhibit proteinase-K. The mitoplast pellets were then washed once in 0.75 mL storage buffer containing 5 mM PMSF and then once in 0.75 mL storage buffer without PMSF. Each time the pellets were spun at 13 000 g for 2 min at 4°C and the supernatants discarded. Finally, the mitoplast pellets were resuspended in 40 μL storage buffer.

The following 4 different treatments were conducted in triplicate on 40 μg of protein from mitochondria or mitoplasts that were obtained from the hindlimb muscle of a single animal. All four treatments included 120 μg/mL RNase-A (cat# 19101, Qiagen, Hilden, Germany) incubation for 30 min on ice.

1. MitoProK: Mitochondria from magnetic-bead IP, +RNase-A (followed by 20 μg/mL proteinase-K).
2. MitoRNase: Mitochondria from magnetic-bead IP, +RNase-A (no proteinase-K).
3. MitoplastRNase: Mitoplasts, +RNase-A (no proteinase-K).
4. CrudeMito: Mitochondria from differential centrifugation, +RNase-A (no proteinase-K).

After RNase-A incubation, either proteinase-K (final concentration 20 μg/mL) or a similar volume of buffer was added to the respective treatment groups and incubated on ice for 30 min. Each tube was then centrifuged at 13 000 g for 2 min at 4°C. The supernatant was aspirated, and the pellet was washed once with 500 μL and then once with 200 μL ice-cold storage buffer. The mitochondrial pellets were resuspended in 400 μL Tri-reagent and frozen at −80°C until RNA extraction.

For RNA extraction, frozen samples were thawed and then pipette mixed thoroughly to disrupt the pellets and then centrifuged at 13 000 g for 10 min. RNA extraction was then performed with on-column DNase I treatment (Zymo Research Direct-zol RNA MicroPrep #2060) and eluted in 12 μL nuclease free water. RNA yield was determined using a TapeStation (Agilent) with High Sensitivity RNA reagents. Mitochondria from magnetic-bead IP yielded ~1.5 ng RNA per μg of protein, whereas mitochondria from differential centrifugation yielded ~0.2 ng RNA per μg of protein.

Total RNA extracted from mitochondria from differential centrifugation (6.3 ng), mitochondria, and mitoplasts

isolated from magnetic-bead IP (40 ng) methods were converted to cDNA libraries (Zymo-Seq RiboFree Total RNA #R300, Zymo Research) and then underwent whole-transcriptome RNA sequencing as described above.

2.13 | Human study ethical approval and procedures

All experimental procedures were approved by the Deakin University Human Research Ethics Committee (DUHREC 2014-096) and conforms to the Declaration of Helsinki. Written, informed consent was obtained from all individuals before participation. Skeletal muscle mitochondria data shown here are a subset of the female cohort ($n = 7$; age, 23.3 ± 3.6 y (mean $\pm$ SD)) previously described by our group.[11]

Skeletal muscle samples were obtained at rest from the vastus lateralis via muscle biopsy using the percutaneous muscle biopsy technique with a Bergstrom needle, modified to include suction.[12,13] Briefly, the skin was anesthetized with 1% Xylocaine, and incisions were made through the skin and muscle fascia. Approximately 60 mg freshly obtained skeletal muscle was blotted free of blood and immediately processed for the isolation of mitochondria. Each skeletal muscle sample was immediately placed in 1 mL ice-cold lysis buffer, minced, and homogenized as described above for rat skeletal muscle. Intact mitochondria were then isolated using the magnetic-bead immunoprecipitation method and RNase-A treatment as described above for rat skeletal muscle mitochondria. The RNase-treated mitochondrial pellet was resuspended in 100 μL storage buffer then frozen at −80°C until RNA extraction.

Frozen mitochondrial pellets were thawed in 5× volumes of TRI-Reagent (Qiagen Inc.) and sheared through a fine pipette tip 15 times to disrupt the mitochondrial pellet. An enriched small RNA fraction was extracted from the isolated mitochondria using the miRNeasy Mini Kit with on-column DNase-I digest (Qiagen Inc.), with half-volumes of 1-bromo-3-chloropropane substituted in place of chloroform as per the manufacturer's protocol. RNA was eluted in 30 μL Nuclease-Free Water (NFW). Mitochondrial RNA concentration and fragment size were assessed by microfluidic capillary electrophoresis (2100 BioAnalyzer Small RNA Chips, Agilent Technologies).

400 pg RNA from the RNase-treated mitochondria samples was reverse-transcribed to first-strand cDNA in a 20 μL reaction along with no-template and no-amplification controls (Applied Biosystems High Capacity RT kit #4368814). The RT protocol consisted of 10 min at 25°C, 120 min at 37°C, and 5 min at 85°C. Quantitative PCR was performed in triplicate (Agilent AriaMX G8830A). cDNA was diluted 1:5 before

nuclear- (*COX4I1*) and mitochondrial-encoded (*MT-CO1, MT-RNR1*, and *MT-RNR2*) transcript abundance was assessed via qPCR using TaqMan hydrolysis probes Cat # 4331182 and TaqMan Universal Master Mix II, no UNG (Table 2). Thermal conditions used for qPCR were 10 min at 95°C (activation) and then 40 cycles of 15 s at 95°C (denature) and 60 s at 55–60°C (anneal/extend).

Once the purity of the isolated human skeletal muscle mitochondria samples was confirmed, mitochondrial miRNA expression was assessed via qPCR. MiR-1, miR-133a, miR-133b, and miR-206 were selected for investigation. 750 pg mitochondrial RNA was first reverse-transcribed in a 20 μL reaction containing TaqMan 5× primers alongside no-template controls (Applied Biosystems miRNA Reverse Transcription Kit #4366596). The RT product was diluted 1:3 in NFW before miRNA transcript abundance was assessed using TaqMan miRNA hydrolysis probes (Table 3) alongside no-amplification and no-template controls using TaqMan Universal Master Mix II, no UNG and TaqMan 20× Assays. miRNA qPCR was performed in triplicate. Thermal conditions used for qPCR were 10 min at 95°C (activation) and then 40 cycles of 15 s at 95°C (denature) and 60 s at 55–60°C (anneal/extend). Quantification cycle (C_q) thresholds were calculated using software (Agilent Aria v1.5) expressed after linear transformation.

2.14 | Statistical analysis

Small RNA-seq data were analyzed by paired t-test. RNase-A dose–response data were tested for normality of variance and then analyzed by one- or two-way ANOVA with Tukey's post hoc test for multiple comparisons using GraphPad Prism (v7). All data are presented as mean (SD) with significance accepted at $p < .05$.

TABLE 2 TaqMan hydrolysis probes used for qPCR on human mitochondria samples.

Gene	GenBank/RefSeq	Assay ID
MT-RNR1	NC_012920.RNR1.0	Hs02596859_g1
MT-RNR2	NC_012920.RNR2.0	HS02596860_s1
MT-CO1	NC_012920.CO1.0	Hs02596864_g1
COX4I1	NM_001861.4	Hs00971639_m1

TABLE 3 TaqMan miRNA hydrolysis probes used for qPCR on human mitochondria samples.

3 | RESULTS

3.1 | Protease purification of isolated mitochondria from myoblasts

We first isolated mitochondria from cultured L6 rat myoblasts using an antibody against an outer mitochondrial membrane protein (TOMM22) conjugated to magnetic beads allowing for precipitation of intact isolated mitochondria (Figure 1). The function, purity, and enrichment of mitochondria using this approach compare favorably to alternatives such as ultracentrifugation and differential centrifugation.[14–16] In the present study, immunoblot of the post-precipitation mitochondrial fraction revealed that a small amount of α-tubulin and Lamin B1 (used as protein markers of the cytosol and nucleus, respectively) were present in the isolated mitochondria fraction (Figure 2, lane 1). A portion of the isolated mitochondria was incubated with the serine protease, proteinase-K, to digest proteins not located within the mitochondrial intermembrane space (IMS) or matrix compartments. This led to depletion of α-tubulin and Lamin B1, in addition to a marker of the outer mitochondrial membrane (TOMM20), while intermembrane space (cytochrome-*c*) and matrix protein markers (citrate synthase) were protected from digestion (Figure 2, lane 2). All proteins probed were susceptible to proteinase-K when mitochondrial membranes were dissolved in the presence of the detergent Triton X-100 (Figure 2, lane 3). Together, this demonstrates that mitochondrial isolation by TOMM22-immunoprecipitation followed by enzymatic treatment yields a purified, intact mitochondrial fraction suitable for downstream protein analyses. Based on this, we hypothesized that an analogous approach utilizing a ribonuclease could be used to remove RNA located outside of isolated mitochondria.

3.2 | Ribonuclease purification of isolated mitochondria from myoblasts

Next, mitochondria isolated from L6 rat myoblasts were exposed to a range of concentrations of RNase-A, an endonuclease that cleaves phosphodiester bonds after pyrimidine residues in the RNA molecule.[17] RNase-A-treated isolated mitochondria were assessed by RT-qPCR for abundance

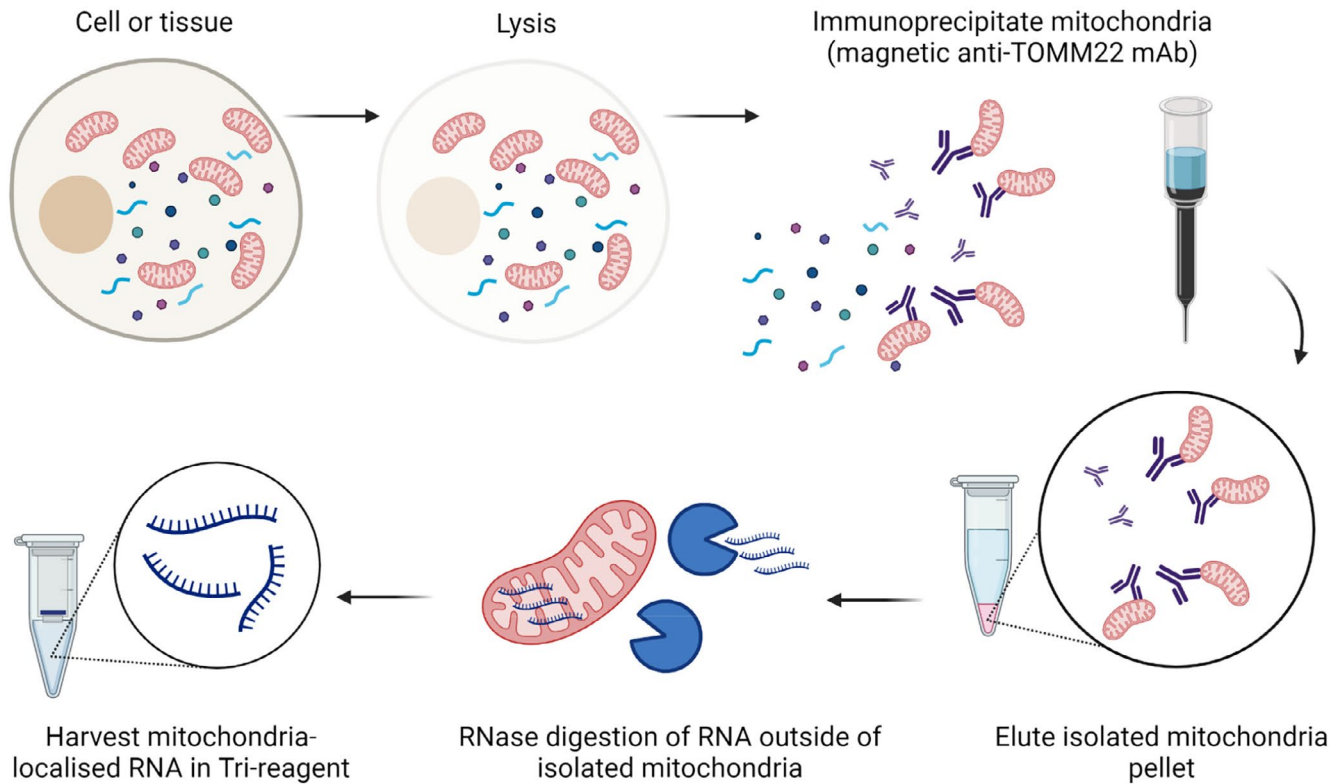| Gene	Mature miRNA sequence	Assay ID
hsa-miR-1	UGGAAUGUAAAGAAGUAUGUAU	002222
hsa-miR-133a	UUUGGUCCCCUUCAACCAGCUG	002246
hsa-miR-133b	UUUGGUCCCCUUCAACCAGCUA	002247
hsa-miR-206	UGGAAUGUAAGGAAGUGUGUGG	000510

FIGURE 1 Overview of TOMM22 immunoprecipitation-based method for mitochondrial isolation.

of mtDNA-encoded mRNA (*Mt-co3*) localized exclusively within the mitochondrial matrix compartment and a nuclear-encoded mRNA (*Cox4i1*) that localizes outside mitochondria.[18] We found that *Mt-co3* was protected from degradation at RNase concentrations up to at least 100 µg/mL, whereas partial *Cox4i1* degradation occurred at 10 µg/mL and was mostly degraded at 100 µg/mL (Figure 3). In the presence of detergent to disrupt mitochondrial membranes, 1 µg/mL RNase-A was sufficient to digest all *Cox4i1* and *Mt-co3*, as well as an exogenous mRNA spike-in control (Figure 3). This suggests that a certain proportion of cytosolic *Cox4i1* is protected from digestion at lower RNase-A concentrations, potentially as a result of being bound to ribosomes at the outer mitochondrial membrane.[19] Taken together, these data suggest that TOMM22-IP mitochondrial isolation followed by RNase-A treatment is suitable for downstream mitochondrial RNA analyses provided the RNase-A concentration is sufficient to remove transcripts not located within the mitochondrial membranes.

3.3 | Small RNA sequencing on purified isolated mitochondria from myoblasts reveals mitochondria localized miRNAs

We next aimed to optimize a protocol to perform transcriptomic analysis of the small RNAs (sRNA) contained
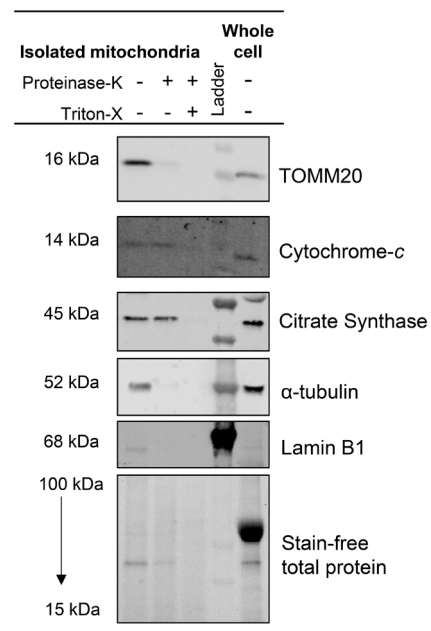

FIGURE 2 Protease treatment of mitochondria isolated from L6 myocytes. Isolated mitochondria were incubated with or without proteinase-K (20 µg/mL) and detergent (1% Triton X-100). Mitochondria (0.2 µg total protein) and whole cell lysate (12 µg total protein) were resolved via SDS-PAGE and probed for marker proteins of subcellular compartments: TOMM20 (OMM), Cytochrome-c (IMS), citrate synthase (matrix), α-tubulin (cytosol), and lamin B1 (nucleus). Blots are representative of $n = 2$ technical replicates from a single mitochondrial isolation preparation.
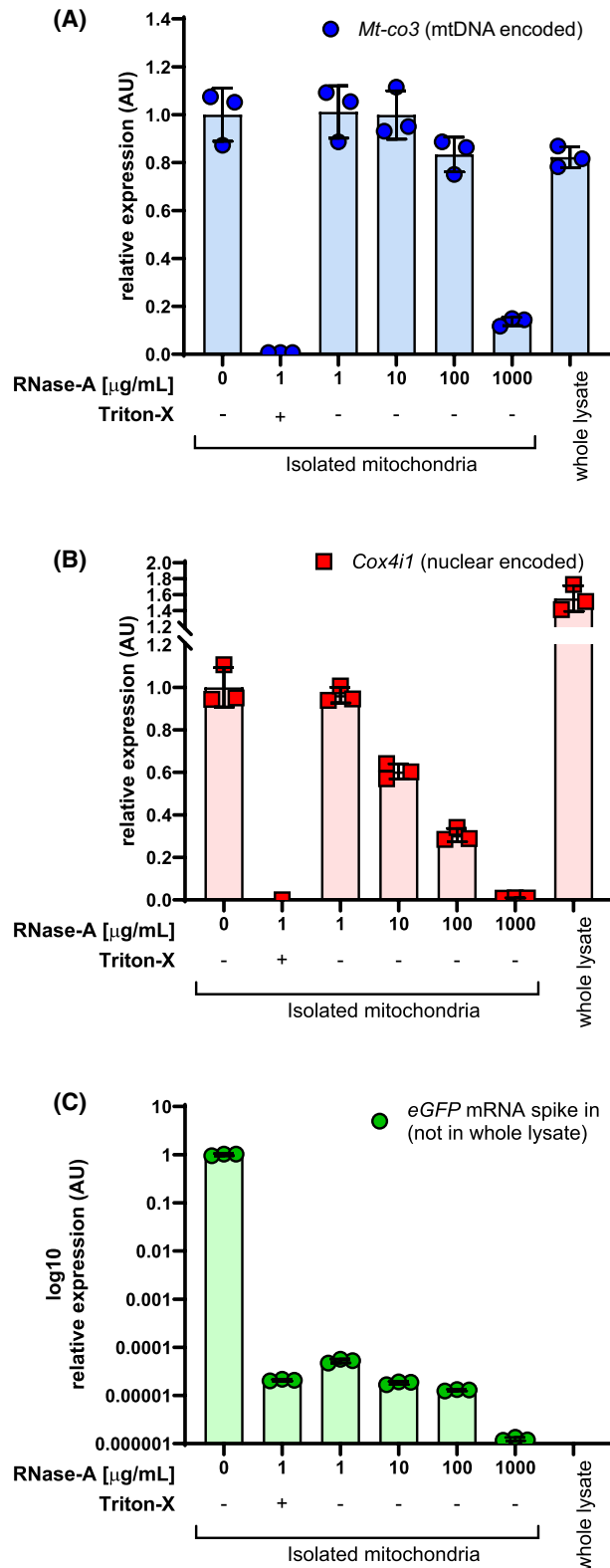
FIGURE 3 RNase-A treatment of mitochondria isolated from L6 myocytes. Isolated mitochondria were incubated with or without RNase-A (1–1000 µg/mL) in the presence or absence of detergent (1% Triton X-100). The levels of representative (A) mtDNA (*Mt-co3*)- and (B) nuclear (*Cox4i1*)-encoded genes were then assessed by RT-qPCR in addition to (C) an exogenous mRNA spike-in control (*eGFP*) added to isolated mitochondria (but not to the whole cell lysate). The values were derived by exponential transformation of the C_q value, and data for each gene are expressed as a fraction of the untreated isolated mitochondria condition (relative expression). Data are mean (SD) for $N = 3$ technical replicates from a single mitochondrial isolation preparation.

Biolabs)). The standard protocol produced large amounts of adapter-dimer and was not sufficient to ligate adapters to the target miRNAs within the sample (Figure 4A,B). We next decreased the amount of the 3′ and 5′ adapters to investigate whether a lower molar ratio improved miRNA ligation efficiency. Both the modified-0.3× (Figure 4C) and modified-0.1× (data not shown) approaches produced quantifiable amounts of the target miRNA library when prepared from 60 ng mitochondrial RNA, although the total cDNA yield was approximately 7-fold higher from the modified-0.3× when compared to modified-0.1× protocol. Both modified approaches did decrease, but not prevent, adapter-dimer formation.

While 60 ng mitochondrial RNA is below the recommended library RNA input (>100 ng, NEBiolabs, Inc.), mitochondrial RNA yield from cell and tissue samples is often considerably below this threshold. Thus, it was necessary to investigate whether the modified-0.3× and modified-0.1× approach could similarly produce the target miRNA library when prepared from much lower amounts of mitochondrial RNA. The modified-0.3× (Figure 4C,D) and modified-0.1× (data not shown) approaches both produced the target library when prepared from >1.8 ng (range 1.8–60 ng) mitochondria RNA. Total cDNA yields were, on average, 4.3-fold higher ($p < .05$) when using the modified-0.3× protocol compared to the modified-0.1×. The presence of adapter-dimer dominated each library, regardless of the mitochondrial RNA input amount used. To combat this, all uniquely indexed libraries were combined in an equimolar pool and run across two lanes of a TBE polyacrylamide gel. The gel fragment corresponding to the miRNA region was manually excised, extracted from the gel and then sequenced. There were no differences in total RNA-seq reads ($p = .79$) and total mapped miRNA reads ($p = .19$) between the modified-0.3× and modified-0.1× protocols (Figure 5A). Over 200 miRNAs were detected across all but the lowest (1.8 ng, modified-0.1×) mitochondrial RNA inputs (Figure 5B). The

within isolated mitochondria from L6 rat myoblasts. We first prepared sRNA cDNA libraries from 120 to 60 ng mitochondrial RNA with 0.5× adapter dilutions (NEBNext 3′ and 5′ SR Adaptors, and RT primer for Illumina), in line with the standard manufacturer protocol (NEBNext Multiplex Small RNA Library Prep Set (New England
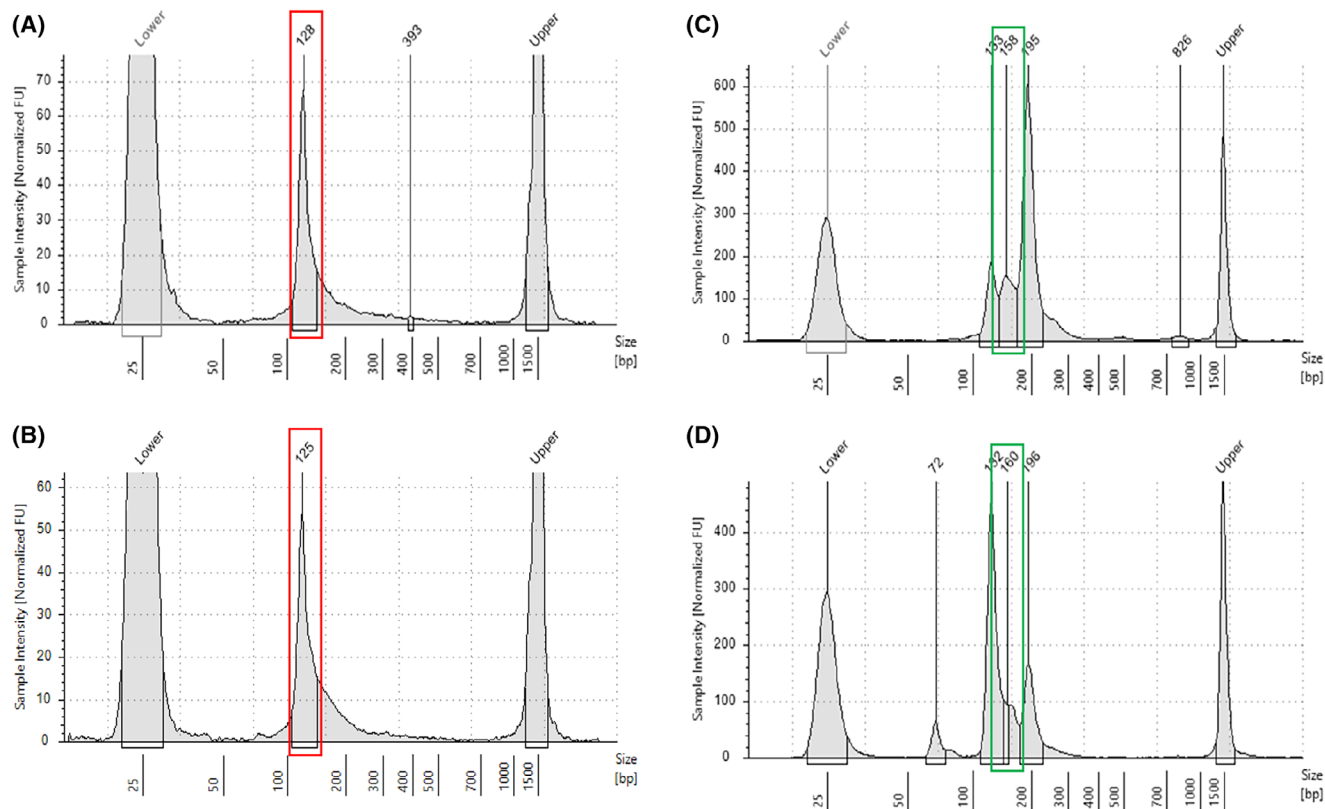
FIGURE 4 Small RNA-seq library preparation from mitochondrial RNA. Representative electropherogram traces of libraries generated with the standard 0.5× dilution of 3′ and 5′ adapters produce large amounts of adapter-dimer (red box) and do not ligate to mitochondria miRNAs with either (A) 120 ng or (B) 60 ng mitochondrial RNA input. Lower molar ratios (0.3× dilution) of 3′ and 5′ adapters produce the target miRNA library (green box) with (C) 60 ng and (D) 1.8 ng mitochondria RNA. Peaks at 25 and 1500 bp are internal size standards.

number of miRNAs detected appeared to plateau when libraries were prepared from 15 to 60 ng mitochondrial RNA (Figure 5B) and suggests that RNA inputs of at least 15 ng are sufficient to detect most miRNAs within a sample. Ultimately, either modified approach is suitable for the construction of miRNA libraries. However, the significantly higher library yields make the modified-0.3× approach amenable to library pooling, gel excision, and subsequent sequencing.

We next investigated the relative abundance of miRNAs sequenced from serial dilutions of mitochondrial RNA input (1.8–30 ng), when compared to the highest mitochondria RNA input (60 ng). Most miRNAs detected were common between libraries prepared from 60 ng mitochondria RNA and the lower mitochondria RNA inputs (Figure 5C–E). Further to this, the relative abundance of miRNAs was comparable between libraries prepared from the two highest RNA inputs (60 vs. 30 ng; Figure 5E). A small number of miRNA species were overrepresented (8 miRNAs) and underrepresented (5 miRNAs) within libraries prepared from the highest RNA input (60 ng) when compared to lowest RNA input (1.8 ng; Figure 5C). MiRNAs detected in the highest, but not lowest, RNA input

displayed low expression levels within the 60 ng sample and together constituted a small proportion (1069 rpm) of total reads. Interestingly, the skeletal muscle-enriched miR-1, miR-133a, miR-133b and miR-16 and miR-486, predicted to have roles in the regulation of mitochondrial function,[20,21] were detected at higher mitochondria RNA inputs (60 and 30 ng), but not lower inputs (1.8–15 ng; Figure 5). In contrast, the let-7 family and the skeletal muscle-enriched miR-206 were highly abundant in all samples and together constituted $63 \pm 8\%$ of all mapped miRNA reads. Importantly, the relative distribution of miRNAs within each sample provides adequate representation across serial dilutions of mitochondrial RNA, making it possible to accurately investigate differential miRNA expression across unique cell and tissue samples with variable mitochondrial RNA yields.

Together, these data suggest that careful optimization is required when preparing sRNA libraries from low amounts of RNA from purified mitochondria. To minimize adapter-dimer presence in sRNA libraries, gel excision and purification of the target miRNA fraction are recommended. Importantly, our data demonstrate that RNA-seq results were comparable across serial dilutions of
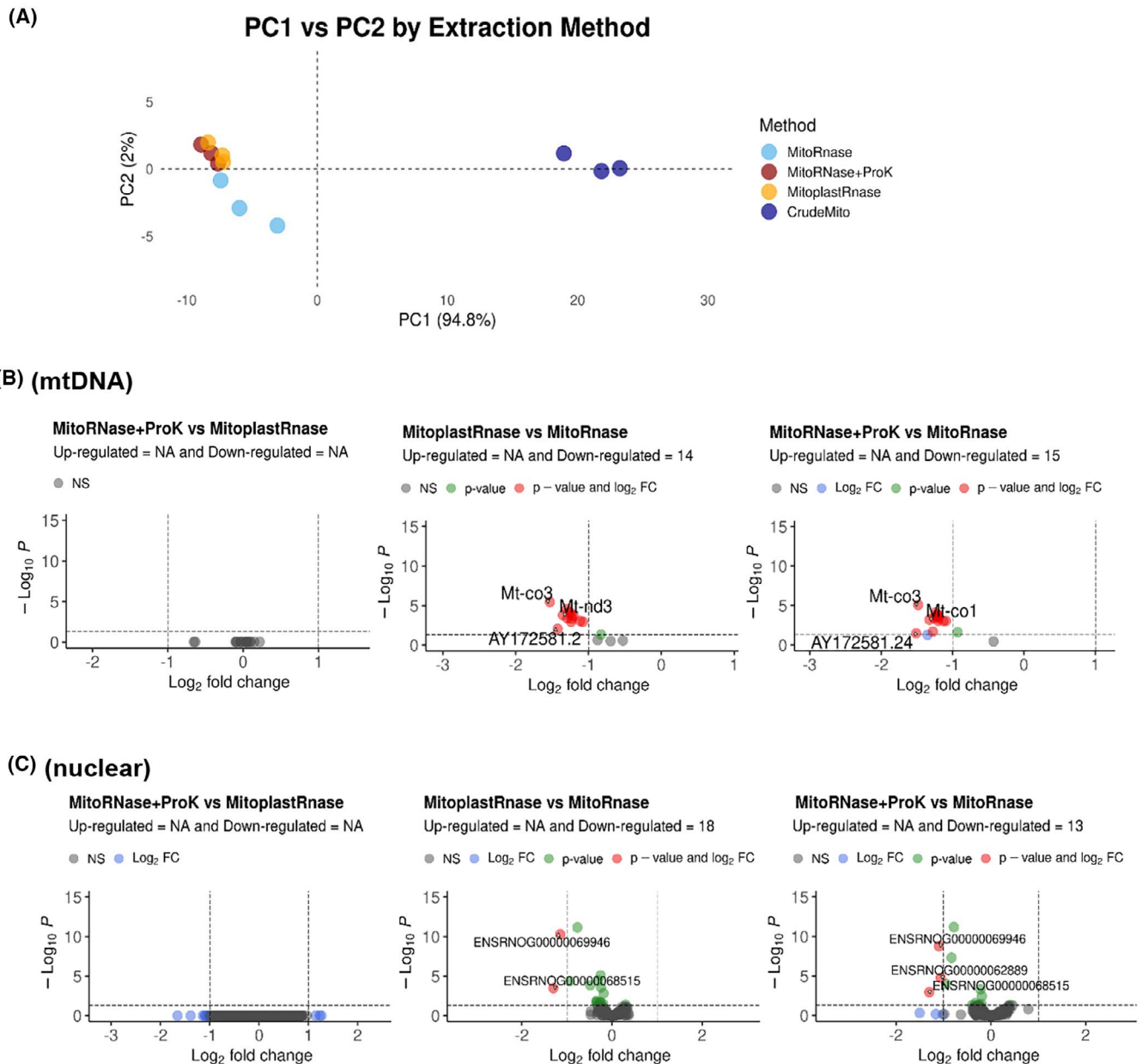
FIGURE 5 Small RNA-Seq on isolated mitochondria from L6 myocytes. (A) Small RNA libraries were prepared from 1.8 to 60 ng mitochondria RNA with modified-0.3× ($n = 6$) or modified-0.1× ($n = 4$) protocols. The total number of reads ($p = .79$) and total mapped miRNA reads ($p = .19$) were not different between protocols. Student's paired t-test, $n = 1$ at each RNA input. (B) Neither mitochondrial RNA input nor library preparation protocols limit the number of mature miRNAs that can be detected from mitochondrial RNA. The number of mature miRNA species detected across all mitochondria RNA inputs was not different ($p = .60$, Student's paired t-test) following modified-0.3× (m-0.3×; $n = 6$) and modified-0.1× (m-0.1×; $n = 4$) protocols. Each point represents an independent library prepared from 1.8 to 60 ng mitochondrial RNA. (C–E) The relative abundance of miRNAs within each sample is comparable between small RNA libraries prepared from high, moderate and low mitochondrial RNA inputs. Venn diagrams depicting unique and shared miRNAs detected from 60 ng mitochondria RNA when compared to (C) 1.8 ng, (D) 7.5 ng, and (E) 30 ng mitochondria RNA, prepared using the modified-0.3× library preparation approach. The relative distribution of miRNAs detected at each RNA input was expressed relative to miR-let-7c-2. Differences in the relative distribution of miRNAs between the highest RNA input and serial RNA dilutions are depicted by gray dots (<5-fold change when compared to 60 ng), red dots (>5-fold change when compared to 60 ng), and green dots (>10-fold change when compared to 60 ng). Highly abundant miRNAs across all RNA inputs (including the let-7 family and mmu-miR-206) are shown in orange dots.

mitochondrial RNA input, suggesting that low mitochondria RNA input does not limit the number nor the relative distribution of miRNA species that can be detected.

3.4 | The transcriptomic profile of enzymatically treated isolated mitochondria from rat skeletal muscle tissue reveals a similar degree of purity as mitoplasts

Next, we applied the purification strategies described thus far to study the transcriptome of mitochondria isolated from muscle tissue samples. From a pooled homogenate of rat skeletal muscle tissue, we compared mitochondria isolated with our IP+enzymatic treatment

method against mitochondria isolated using a traditional differential centrifugation method. At the protein level, mitochondria isolated by immunoprecipitation had no detectable ribosomal marker proteins and very little abundance of peroxisome, Golgi apparatus, or endoplasmic reticulum marker proteins, which contrasted with mitochondria obtained via the differential centrifugation method (Figure 6A,B). Next, to confirm the lack of co-purifying contaminants on the outer mitochondrial membrane, we compared our IP isolated+enzymatic treated mitochondria with mitoplasts (i.e., mitochondria whose OMM is removed or disrupted but with an IMM and matrix that remains intact). We generated mitoplasts and confirmed that they were devoid of outer mitochondrial membrane (OMM) proteins such as

FIGURE 6 Purity of mitochondria isolated by magnetic-bead immunoprecipitation and creation of mitoplasts. (A) Immunoblots for various subcellular marker proteins of ribosomes (S6 RPL) and peroxisomes (Catalase), outer mitochondrial membrane (TOMM20). (B) Golgi apparatus (GM130) and endoplasmic reticulum (ER, SERCA1) and the mitochondrial matrix (Citrate Synthase). Samples are whole cell lysate (WCL, 6 μg total protein) along with isolated mitochondria (6 μg protein) from two independent preparations (two technical replicates) from the same rat skeletal muscle hindlimb obtained using the magnetic-bead immunoprecipitation method (IP) treated with or without 20 μg/mL proteinase-K, and differential centrifugation (crude mitochondria, CM, 6 μg total protein), as described in *Methods*. (C) Mitoplasts were created from isolated mitochondria (40 μg of protein) by incubating with increasing amounts of digitonin (0.0%–0.40% final concentration) for 30 min at 4°C followed by 20 μg/mL proteinase-K for 30 min at 4°C. The amount of total protein loaded for the digitonin-treated mitochondria, CM, and WCL was 6, 4, and 8 μg, respectively. Marker proteins of subcellular compartments were then probed in the mitochondrial pellets and in the supernatants by immunoblot. Blots are representative of digitonin treatments from a single mitochondrial isolation preparation (single replicate).

(A)

(B) (mtDNA)

(C) (nuclear)

FIGURE 7 Mitoplasts and enzymatically treated isolated mitochondria from rat skeletal muscle tissue have a similar RNA transcriptome. (A) PCA plot of RNA-seq whole transcriptome of mitochondria isolated via IP, RNase-A treated, then treated with proteinase-K ("MitoRnase+ProtK") or without ("MitoRnase"), mitoplast preparations treated with RNase-A ("MitoplastRnase"), and crude mitochondria extracts isolated by differential centrifugation treated with RNase-A ("CrudeMito"). Data are $N = 3$ technical replicates (independent mitochondrial isolation procedures), from the tissue of $n = 1$ animal. Volcano plots of differentially expressed (B) mtDNA-encoded genes and (C) nuclear-encoded genes between the different mitochondrial treatments and mitoplasts, statistical significance accepted at adjusted p-value (FDR) <.05 and $\log_2$ fold-change <1.

TOMM20 and inner mitochondrial membrane (IMM) and inter membrane space (IMS) proteins such as mitofilin and AIF without the loss of mitochondrial matrix proteins such as citrate synthase (Figure 6C).

We then performed RNA-sequencing on four different mitochondrial sample types: (i) RNase-A treated mitoplasts, (ii) RNase-A treated IP isolated mitochondria with or (iii) without proteinase-K enzymatic purification (to evaluate RNAs that may be bound to ribosomes on the OMM or other RNA binding proteins which protect them from RNase-A), and (iv) RNase-A treated mitochondria isolated via differential centrifugation ("CrudeMito"). Principal component analysis of the transcriptomes of these mitochondrial sample types revealed a separation along the first principal component between crude mitochondria extracts isolated by differential centrifugation ("CrudeMito") compared with mitochondria isolated via IP and treated with
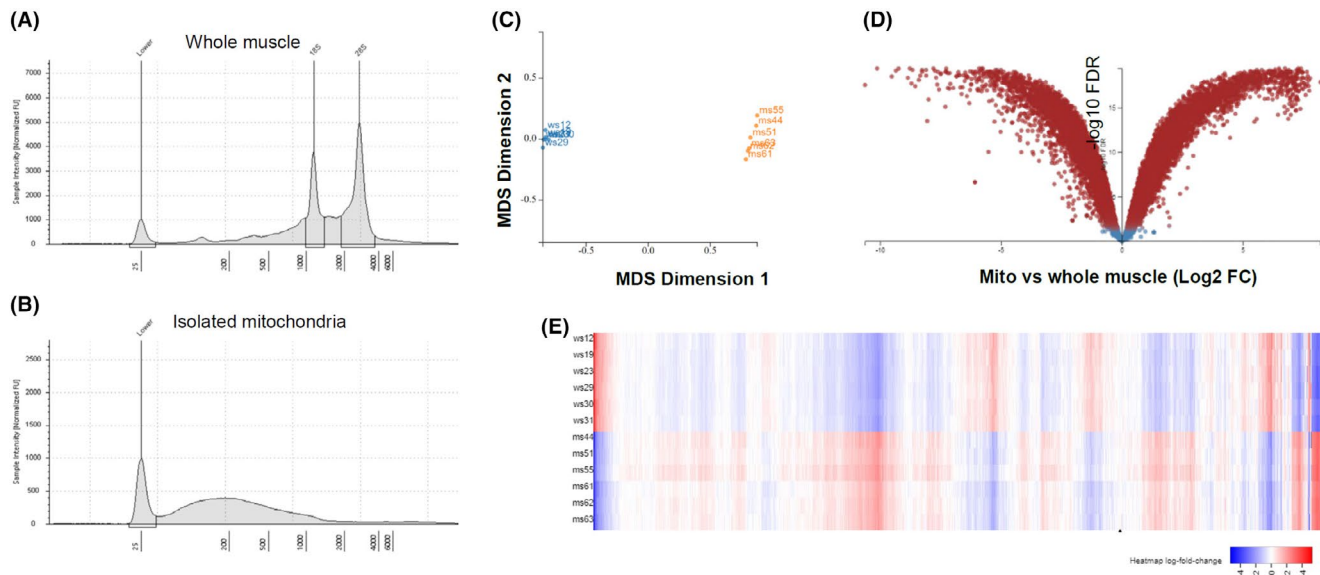
FIGURE 8 RNA from enzymatically treated isolated mitochondria from rat skeletal muscle and respective whole muscle tissue. Representative gel electropherogram traces of RNA extracted from (A) whole muscle and (B) RNaseA+ProtK treated isolated mitochondria, note the expected absence of ribosomal peaks in the mitochondrial sample. Peak at 25 nt is an internal size standard. (C) Multidimensional scaling plot of whole muscle (blue) and mitochondrial libraries (orange). (D) Volcano plot of genes with higher abundance in mitochondria (positive values) compared to whole muscle (red points: FDR ≤ 0.05). (E) Heatmap of gene expression levels in whole muscle samples (top half) relative to the respective isolated mitochondria (bottom half) for 12 093 transcripts with ≥1 CPM from $n = 6$ biological replicates.

RNase-A and with or without proteinase-K treatment (MitoRNase+ProtK and MitoRNase, respectively) or mitoplasts treated with RNase-A ("MitoplastRNase") (Figure 7A). The overlap of the latter three suggests a high overall degree of similarity of the transcriptomic profile between immunoprecipitation-based methods when compared to the crude mitochondrial fraction. For this reason, the crude mitochondrial fraction was excluded from further analysis.

There were no differentially expressed (DE) mtDNA-encoded genes (Figure 7B left panel) or nDNA-encoded genes between MitoplastRNase and MitoRNase+ProtK (Figure 7C left panel). In contrast, there were several DE genes (both mtDNA- and nDNA-encoded) between MitoRNase without proK and MitoplastRNase (Figure 7B,C middle panel), and also between MitoRNase without proK and MitoRNase+ProtK (Figure 7B,C right panel). The same pattern was observed for mtDNA- and nDNA-encoded rRNAs and mitochondrial tRNAs (data not shown). Collectively, these data demonstrate that mitochondria isolated via our method of immunoprecipitation followed by RNase-A and proteinase-K treatments yield a transcriptome of similar purity to that of mitoplasts.

Next, we extracted RNA from IP+purified (RNase + ProtK) mitochondria and RNA from the corresponding whole tissue from the gastrocnemius skeletal muscle of 9-week-old rats (Figure 8A,B). Whole-transcriptome RNA sequencing (Figure 8C–E) revealed that the transcriptomes of these mitochondria had a high degree of purity

as indicated firstly by a low relative proportion of nuclear-encoded mRNAs unrelated to mitochondria, such as genes associated with muscle sarcomere function, that is, myosin light (e.g., *Myl1*) and heavy (e.g., *Myh4* and *Myh7*) isoforms, α-actin (*Acta1*) and troponins (e.g., *Tnnc2*, *Tnnt3*; Figure 9A). Secondly, the mitochondrial fraction also contained a low relative abundance of nuclear-encoded OXPHOS genes (including *Cox4i1*), as expected (Figure 9B). Thirdly, there was similar abundance of all mtDNA-encoded OXPHOS mRNA transcripts including *Mt-co3* between the whole tissue and mitochondrial fractions (Figure 9C). This serves as an important internal control as mtDNA transcripts are expected to be present in both isolated mitochondria and whole tissue in similar proportions.

Lastly, we confirmed the suitability of this approach with human muscle tissue biopsy samples. We isolated and purified mitochondria from these samples and performed analysis via RT-qPCR. This revealed the absence of *COX4I1*, used as marker of nuclear-encoded mRNA contamination, yet, several muscle-enriched miRNAs including miR-206 were detected (Table 4), which is consistent with our results in L6 myoblasts.

4 | DISCUSSION

Studies of subcellular fractions using high-throughput analyses require careful consideration of purification

FIGURE 9 Purity of enzymatically treated isolated mitochondria from rat skeletal muscle relative to respective whole muscle tissue. Whole-transcriptome RNA sequencing of isolated mitochondria and respective whole muscle tissue (rat gastrocnemius) shows that the isolated mitochondria were free of (A) highly abundant muscle sarcomere-related mRNAs and (B) and nuclear-encoded mRNAs involved in the mitochondrial electron transport chain, while (C) mtDNA-encoded mitochondrial electron transport chain genes were present. Each point represents the mean normalized abundance (counts per million, CPM) of an individual gene from $n=6$ animals.
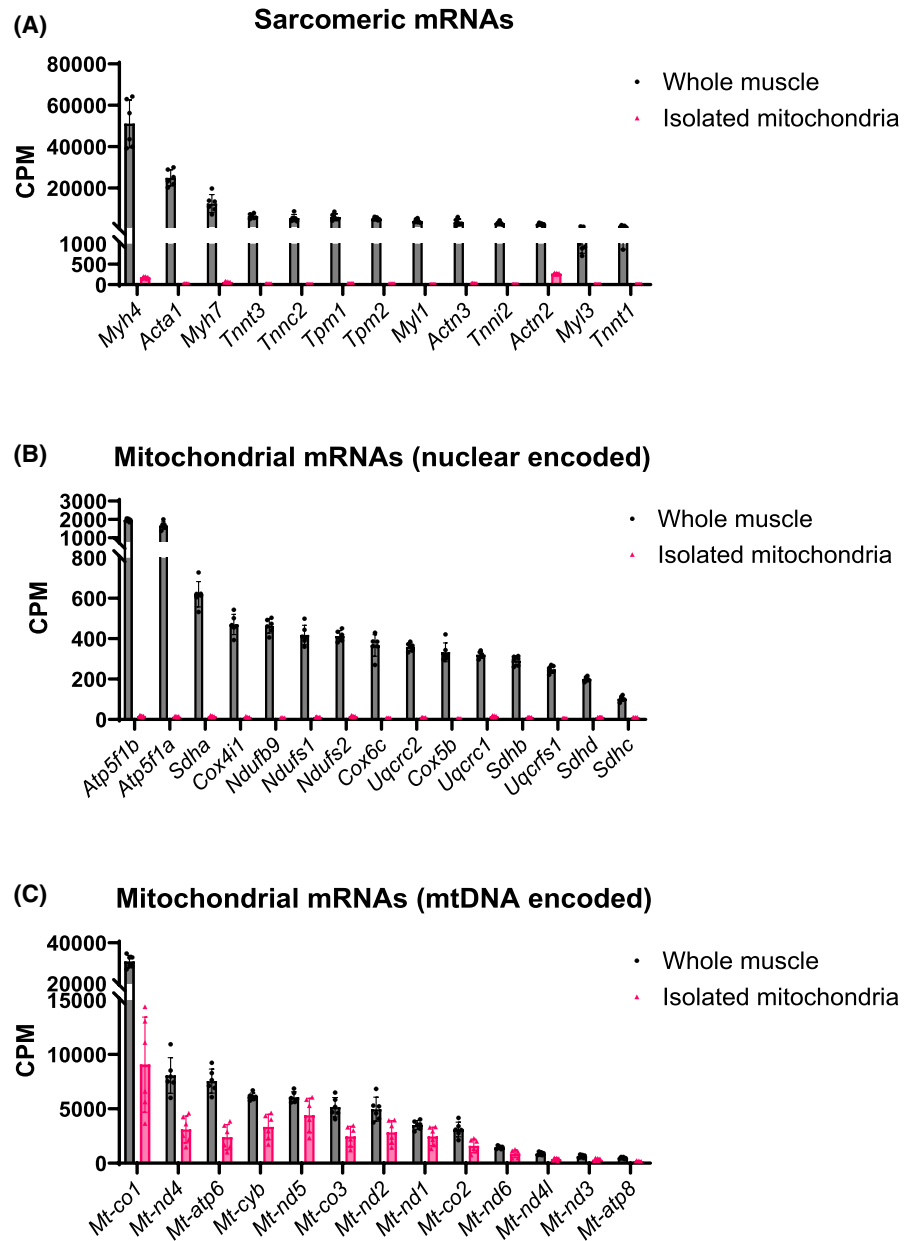
strategies to avoid confounding effects of contaminants. Here, we report an optimized method for purification of isolated mitochondria for downstream transcriptomic analysis. Revealing the utility of this approach, we confirmed that miRNAs can be reliably detected in the mitochondria of L6 myoblasts even when libraries are prepared from RNA inputs well below the thresholds often recommended by manufacturers.

Incubation of isolated mitochondria with RNase-A digests any contaminating extra-mitochondrial RNA to ensure that only RNA species contained within the mitochondria membranes are identified in downstream analyses. This is important when investigating transcripts that do not localize in one subcellular compartment, but instead may be actively transported between compartments in response to various physiological stimuli. RNase-A protocols differ substantially between studies that have investigated mitochondrial RNA expression. In previous studies, RNase-A has been used at variable final concentrations (5–50 μg/mL)[2,22–24] or has been omitted entirely.[3,4,25,26] Here, we demonstrate that RNase-A concentrations of at least 100 μg/mL are required to digest the majority of nuclear-encoded transcripts (such as *Cox4i1*) in rat myoblasts. Importantly, this approach is transferable between cell and tissue models and is shown to effectively degrade potentially contaminating, non-mitochondrial RNA in mitochondria isolated from human skeletal muscle tissue (Table 4).

Investigations into the mitochondrial RNA population are often limited by technical challenges. For example, the inherently low mitochondrial RNA yields compared to

TABLE 4 Mitochondria from human skeletal muscle contain miRNA.

Transcript	Description	C_q from mitochondrial RNA extract
MT-CO1	Mitochondrial gene marker	22.3 ± 2.5
MT-RNR1	Mitochondrial 12S ribosomal RNA	19.4 ± 2.7
MT-RNR2	Mitochondrial 16S ribosomal RNA	21.1 ± 2.0
COX4I1	Nuclear gene marker	Not detected
miR-1	Muscle-enriched miRNA	30.8 ± 0.8
miR-133a	Muscle-enriched miRNA	28.7 ± 0.8
miR-133b	Muscle-enriched miRNA	30.0 ± 0.8
miR-206	Muscle-enriched miRNA	30.0 ± 1.7

Note: Total RNA from isolated mitochondria was extracted, reverse-transcribed (400 pg per reaction for mRNA analyses; 750 pg per reaction for miRNA analyses), and then assessed via qPCR. RNA was free of nuclear-encoded transcripts, abundant in mitochondrial genome specific transcripts, and also contained miRNAs. Quantification cycle (C_q) values are mean $\pm$ SD for isolated mitochondrial preparations from skeletal muscle of $n = 7$ healthy female volunteers.

total cellular RNA are well below the threshold required for commercially available small RNA library preparation protocols. This challenge may be overcome by combining mitochondria RNA from biological samples into pools that represent a single "intervention" or "clinical" group and the "control" group.[27,28] While this effectively increases the amount of mitochondrial RNA available for sRNA library preparation, this approach introduces further limitations. First, the use of pooled samples requires a much larger sample size to achieve the same statistical power.[29] Second, gene expression is highly variable between individuals; taking a pooled sample approach may mask potential individual variability in miRNA expression.[29,30] Our findings illustrate that small RNA libraries can be prepared from individual biological samples without the need to pool multiple samples, thereby increasing the statistical power available, especially for human studies with limited sample material and high participant burden.

A modified small RNA library preparation protocol increased ligation efficiency of the 3′ and 5′ adapters to miRNAs within mitochondrial samples. However, this modified approach was not able to prevent adapter-dimer formation entirely. As the adapter-dimer product is approximately 20 bp smaller than adapter-ligated miRNAs and preferentially binds to the flow cell during RNA-Seq, gel extraction of the target miRNA region is essential to maximize read counts that map to miRNAs rather than adapter-dimer.[31] When used together, the modified-0.3× protocol plus gel extraction were successful in detecting over 200 miRNAs from

L6 mitochondria RNA inputs as low as 1.8 ng. Importantly, the relative distribution of miRNAs within each sample was reasonably consistent as RNA input decreased. However, some miRNA species tended to be overrepresented at the lowest mitochondria RNA inputs. This may be because there were less miRNA species detected in the library prepared from 1.8 ng (207 miRNAs) when compared to 60 ng mitochondria RNA (266 miRNAs). Overall, there appears to be minimal bias toward over- or underrepresenting specific miRNA species at low RNA inputs.

Of note, the skeletal muscle-enriched miR-1, miR-133a, and miR-133b were detected at high (30 and 60 ng) but not low (1.8–15 ng) mitochondrial RNA inputs. MiR-1 and miR-133a have previously been observed in mitochondria isolated from human skeletal and rodent cardiac muscle cells in vitro.[2,23,27] MiR-1 enhances the translation of the mitochondrial-encoded *Mt-co1, Mt-nd1*, and *Mt-cytb*, among others,[23] while deletion of miR-133a inhibits the transcription of nuclear-encoded genes including *Ppargc1a* and *Tfam*,[32] both of which are upstream regulators of mitochondrial biogenesis. The use of proliferating L6 myocytes in this study, compared with primary human myocytes[2] and rat neonatal cardiomyocytes[23] used previously, may partially account for the differences in miRNA species detected. Although L6 cells have reportedly higher rates of aerobic metabolism when compared to C2C12 cells and primary human myocytes, cell culture models are more dependent upon anaerobic glycolysis.[33] Thus, mitochondrial abundance and function in various cell culture models may differ to those observed with in vivo models. This study was primarily designed to optimize the sRNA-Seq library preparation protocol rather than investigate the physiological relevance of specific miRNAs. Future in vivo studies are now required to profile mitochondrial miRNAs and their roles in tissues that have high bioenergetic requirements such as skeletal and cardiac muscle.

Finally, having a reliable method to discover nuclear-encoded RNAs within mitochondria in response to physiological stimuli will allow for future studies into RNA import and/or regulation at the subcellular level. For instance, noncoding RNAs such as lncRNAs can have important regulatory roles,[34] mediating cellular processes by modulating the expression of genes, stability of transcripts, and/or function of proteins,[35] including those that directly determine mitochondrial function.[36,37] However, only a relatively small fraction (~5%–10%) of all identified lncRNAs have been functionally characterized.[38] Therefore, understanding the subcellular distribution may also open new avenues of investigation into how they are imported into the mitochondrial compartment, what are their putative binding target(s) and whether they modulate expression levels of mtDNA-encoded genes and/or function of mitochondrial proteins. This will be key to understanding

the potential effects on mitochondrial parameters such as oxidative phosphorylation, ROS production, mitochondrial biogenesis, dynamics, or mitophagy.

In summary, we report a method for obtaining a highly pure fraction of mitochondria from cultured myoblasts and skeletal muscle tissue and optimized approach for high-throughput transcriptomic sequencing on this subcellular fraction. Given the increasing interest in RNA-mediated regulation of cellular function in health and disease, future investigations are warranted to better understand the potential biological and physiological significance of the mitochondrial localization of nuclear-encoded RNAs.

AUTHOR CONTRIBUTIONS

Conceptualization: Jessica Silver, Adam J. Trewin, Søren Nielsen, Séverine Lamon, and Glenn. D. Wadley. Conducted experiments: Jessica Silver, Adam J. Trewin, Glenn. D. Wadley, and Stella Loke. Conducted human studies: Jessica Silver, Glenn. D. Wadley, Séverine Lamon, and Hayley Dillon. Data analysis (bioinformatics): Mark Ziemann, Larry Croft, and Megan Soria. Data analysis and visualization: Jessica Silver, Adam J. Trewin, and Megan Soria. Manuscript—original draft: Jessica Silver and Adam J. Trewin. Manuscript—review and editing: Jessica Silver, Adam J. Trewin, Stella Loke, Larry Croft, Mark Ziemann, Megan Soria, Hayley Dillon, Søren Nielsen, Séverine Lamon, and Glenn. D. Wadley. Approved final version of manuscript: Jessica Silver, Adam J. Trewin, Stella Loke, Larry Croft, Mark Ziemann, Megan Soria, Hayley Dillon, Søren Nielsen, Séverine Lamon, and Glenn. D. Wadley.

DISCLOSURES

The authors have stated explicitly that there are no conflicts of interest in connection with this article.

DATA AVAILABILITY STATEMENT

RNA-sequencing datasets from this study have been deposited at the NCBI Gene Expression Omnibus for the small RNA-Seq on isolated mitochondria from L6 myocytes described in Figure 5 (accession number GSE276303); mitoplasts and enzymatically treated isolated mitochondria from rat skeletal muscle described in Figure 7 (accession number GSE276306), and the isolated mitochondria from rat skeletal muscle relative to respective whole muscle tissue in Figure 9 (accession number GSE276307).

ORCID

Jessica Silver https://orcid.org/0000-0002-4654-0868
Adam J. Trewin https://orcid.org/0000-0001-7322-4054
Stella Loke https://orcid.org/0000-0002-5767-6146
Larry Croft https://orcid.org/0000-0002-4588-6170
Mark Ziemann https://orcid.org/0000-0002-7688-6974
Megan Soria https://orcid.org/0000-0002-8715-6854
Hayley Dillon https://orcid.org/0000-0002-3783-7993
Søren Nielsen https://orcid.org/0000-0002-3119-750X
Séverine Lamon https://orcid.org/0000-0002-3271-6551
Glenn D. Wadley https://orcid.org/0000-0002-6617-4359

REFERENCES

1. Spinelli JB, Haigis MC. The multifaceted contributions of mitochondria to cellular metabolism. *Nat Cell Biol*. 2018;20:745-754.
2. Barrey E, Saint-Auret G, Bonnamy B, Damas D, Boyer O, Gidrol X. Pre-microRNA and mature microRNA in human mitochondria. *PLoS ONE*. 2011;6:e20220.
3. Sripada L, Tomar D, Prajapati P, Singh R, Singh AK, Singh R. Systematic analysis of small RNAs associated with human mitochondria by deep sequencing: detailed analysis of mitochondrial associated miRNA. *PLoS ONE*. 2012;7:e44873.
4. Das S, Ferlito M, Kent OA, et al. Nuclear miRNA regulates the mitochondrial genome in the heart. *Circ Res*. 2012;110:1596-1603.
5. Noh JH, Kim KM, Abdelmohsen K, et al. HuR and GRSF1 modulate the nuclear export and mitochondrial localization of the lncRNA RMRP. *Genes Dev*. 2016;30:1224-1239.
6. Silver J, Wadley G, Lamon S. Mitochondrial regulation in skeletal muscle: a role for non-coding RNAs? *Exp Physiol*. 2018;103:1132-1144.
7. Wang G, Chen HW, Oktay Y, et al. PNPASE regulates RNA import into mitochondria. *Cell*. 2010;142:456-467.
8. Zurlo F, Larson K, Bogardus C, Ravussin E. Skeletal muscle metabolism is a major determinant of resting energy expenditure. *J Clin Invest*. 1990;86:1423-1427.
9. Russell AP, Foletta VC, Snow RJ, Wadley GD. Skeletal muscle mitochondria: a major player in exercise, health and disease. *Biochim Biophys Acta*. 2014;1840:1276-1284.
10. Powell D. *Degust v4.1.1*. Zenodo; 2019. doi:10.5281/zenodo.3501067
11. Silver JL, Alexander SE, Dillon HT, Lamon S, Wadley GD. Extracellular vesicular miRNA expression is not a proxy for

skeletal muscle miRNA expression in males and females following acute, moderate intensity exercise. *Physiol Rep*. 2020;8:e14520.

12. Bergström J, Hultman E. The effect of exercise on muscle glycogen and electrolytes in normals. *Scand J Clin Lab Invest*. 1966;18:16-20.

13. Evans WJ, Phinney SD, Young VR. Suction applied to a muscle biopsy maximizes sample size. *Med Sci Sports Exerc*. 1982;14:101-102.

14. Hornig-Do H-T, Günther G, Bust M, Lehnartz P, Bosio A, Wiesner RJ. Isolation of functional pure mitochondria by superparamagnetic microbeads. *Anal Biochem*. 2009;389:1-5.

15. Hubbard WB, Harwood CL, Prajapati P, Springer JE, Saatman KE, Sullivan PG. Fractionated mitochondrial magnetic separation for isolation of synaptic mitochondria from brain tissue. *Sci Rep*. 2019;9:9656.

16. Franko A, Baris OR, Bergschneider E, et al. Efficient isolation of pure and functional mitochondria from mouse tissues using automated tissue disruption and enrichment with anti-TOM22 magnetic beads. *PLoS ONE*. 2013;8:e82392.

17. Witzel H. The function of the pyrimidine base in the ribonuclease reaction. In: Davidson JN, Cohn WE, eds. *Progress in Nucleic Acid Research and Molecular Biology*. Vol 2. Academic Press; 1963:221-258.

18. Suissa M, Schatz G. Import of proteins into mitochondria. Translatable mRNAs for imported mitochondrial proteins are present in free as well as mitochondria-bound cytoplasmic polysomes. *J Biol Chem*. 1982;257:13048-13055.

19. Gold VA, Chroscicki P, Bragoszewski P, Chacinska A. Visualization of cytosolic ribosomes on the surface of mitochondria by electron cryo-tomography. *EMBO Rep*. 2017;18:1786-1800.

20. Nielsen S, Scheele C, Yfanti C, et al. Muscle specific microRNAs are regulated by endurance exercise in human skeletal muscle. *J Physiol*. 2010;588:4029-4037.

21. Russell AP, Lamon S, Boon H, et al. Regulation of miRNAs in human skeletal muscle following acute endurance exercise and short-term endurance training. *J Physiol*. 2013;591:4637-4653.

22. Mercer TR, Neph S, Dinger ME, et al. The human mitochondrial transcriptome. *Cell*. 2011;146:645-658.

23. Zhang X, Zuo X, Yang B, et al. MicroRNA directly enhances mitochondrial translation during muscle differentiation. *Cell*. 2014;158:607-619.

24. Bandiera S, Ruberg S, Girard M, et al. Nuclear outsourcing of RNA interference components to human mitochondria. *PLoS ONE*. 2011;6:e20746.

25. Dasgupta N, Peng Y, Tan Z, Ciraolo G, Wang D, Li R. miRNAs in mtDNA-less cell mitochondria. *Cell Death Dis*. 2015;1:15004.

26. Lung B, Zemann A, Madej MJ, et al. Identification of small non-coding RNAs from mitochondria and chloroplasts. *Nucleic Acids Res*. 2006;34:3842-3852.

27. Jagannathan R, Thapa D, Nichols CE, et al. Translational regulation of the mitochondrial genome following redistribution of mitochondrial microRNA (MitomiR) in the diabetic heart. *Circ Cardiovasc Genet*. 2015;8:785-802.

28. Wang X, Song C, Zhou X, et al. Mitochondria associated microRNA expression profiling of heart failure. *Biomed Res Int*. 2017;2017:4042509.

29. Takele Assefa A, Vandesompele J, Thas O. On the utility of RNA sample pooling to optimize cost and statistical power in RNA sequencing experiments. *BMC Genomics*. 2020;21:312.

30. Rajkumar AP, Qvist P, Lazarus R, et al. Experimental validation of methods for differential gene expression analysis and sample pooling in RNA-seq. *BMC Genomics*. 2015;16:548.

31. Shore S, Henderson JM, Lebedev A, et al. Small RNA library preparation method for next-generation sequencing using chemical modifications to prevent adapter dimer formation. *PLoS ONE*. 2016;11:e0167009.

32. Nie Y, Sato Y, Wang C, Yue F, Kuang S, Gavin TP. Impaired exercise tolerance, mitochondrial biogenesis, and muscle fiber maintenance in miR-133a-deficient mice. *FASEB J*. 2016;30:3745-3758.

33. Abdelmoez AM, Sardón Puig L, Smith JAB, et al. Comparative profiling of skeletal muscle models reveals heterogeneity of transcriptome and metabolism. *Am J Physiol Cell Physiol*. 2020;318:C615-C626.

34. Wadley GD, Lamon S, Alexander SE, McMullen JR, Bernardo BC. Non-coding RNAs regulating cardiac muscle mass. *J Appl Physiol*. 2019;127:633-644.

35. Long Y, Wang X, Youmans DT, Cech TR. How do lncRNAs regulate transcription? *Sci Adv*. 2017;3:eaao2110.

36. Tran KV, Brown EL, DeSouza T, et al. Human thermogenic adipocyte regulation by the long noncoding RNA LINC00473. *Nat Metab*. 2020;2:397-412.

37. Kerr AG, Wang Z, Wang N, et al. The long noncoding RNA ADIPINT regulates human adipocyte metabolism via pyruvate carboxylase. *Nat Commun*. 2022;13:2958.

38. Gao F, Cai Y, Kapranov P, Xu D. Reverse-genetics studies of lncRNAs—what we have learnt and paths forward. *Genome Biol*. 2020;21:93.